# Characterization of Solids in Residual Wastes from Single-Shell Tanks at the Hanford Site, Washington, USA – 9277

Kenneth M. Krupka*, Kirk J. Cantrell*, H. Todd Schaef*, Bruce W. Arey*,
Steve M. Heald**, William J. Deutsch*, and Michael J. Lindberg*
* Pacific Northwest National Laboratory, Richland, Washington 99352
** Argonne National Laboratory, Argonne, Illinois 60439

## ABSTRACT

Solid-phase characterization methods have been used in an ongoing study of residual wastes (i.e., waste remaining after final retrieval operations) from underground single-shell storage tanks 241-C-103, 241-C-106, 241-C-202, 241-C-203, and 241-S-112 at the U.S. Department of Energy's Hanford Site in Washington State. The results of studies completed to date show significant variability in the compositions of those residual wastes and the compositions, morphologies, and crystallinities of the individual phases that make up these wastes. These differences undoubtedly result from the various waste types stored and transferred into and out of each tank and the different sluicing and retrieval operations used for waste retrieval.

The studies indicate that these residual wastes are chemically-complex assemblages of crystalline and amorphous solids that contain contaminants as discrete phases and/or co-precipitated within oxide phases. Depending on the specific tank, various solids (e.g., gibbsite; boehmite; dawsonite; cancrinite; Fe oxides/hydroxides such as hematite, goethite, and maghemite; rhodochrosite; lindbergite; whewellite; nitratine; and numerous amorphous or poorly crystalline phases) have been identified by X-ray diffraction and scanning electron microscopy/energy dispersive X-ray spectroscopy in residual wastes studied to date. The studies also show that contact of residual wastes with $Ca(OH)_2$- and $CaCO_3$-saturated aqueous solutions, which were used as surrogates for the compositions of pore-fluid leachants derived from young and aged cements, respectively, may alter the composition of solid phases present in the contacted wastes.

Iron oxides/hydroxides have been identified in all residual wastes studied to date. They occur in these wastes as discrete particles, particles intergrown within a matrix of other phases, and surface coatings on other particles or particle aggregates. These Fe oxides/hydroxides typically contain trace concentrations of other transition metals, such Cr, Mn, Ni, and/or Pb. Recent analyses of residual waste from 241-C-103 have revealed the presence of Tc-containing Fe oxide/hydroxide particles, which is believed to be the first direct evidence of Tc in solid phases in actual samples of Hanford pre-retrieval tank waste or post-retrieval residual waste. The presence of mineralized coatings, such as Fe oxides/hydroxides or reaction products precipitated from contact with cement pore fluids, on contaminant-containing particles could decrease their rate of dissolution, thereby delaying the release of contaminants until the coatings dissolve sufficiently to expose the underlying matrix to infiltrating pore fluids.

Certain key cross-cutting geochemical processes and solid phase characteristics important to contaminant waste release are becoming evident, now that residual wastes have been studied from several single-shell tanks. As more residual tank wastes are characterized in terms of composition and contaminant release, it is anticipated that common characteristics with respect to the type of wastes stored in the tanks will become evident. This may allow the grouping of tanks into general categories with certain common chemical features and contaminant release characteristics – an important goal because complete characterization of residual wastes from all 149 single-shell storage tanks is not practical. Additionally, information garnered from residual waste characterization activities can be used to optimize future waste retrieval operations.

## INTRODUCTION

Performance assessments [1,2] will be completed to evaluate the long-term health risks associated with closure of 177 single- (SST) and double-shell (DST) underground storage tanks containing residual radioactive and hazardous wastes at the U.S. Department of Energy (DOE) Hanford Site in southeastern Washington state. DOE and its contractors CH2M HILL Hanford Group, Inc. (through September 2008) and Washington River Protection Solutions, LLC (starting October 2008) are in the process of closing these tanks by removing as much of the waste material as technically possible. Progress, methods used, and lessons learned in the retrieval of wastes from Hanford's SSTs through February 2008, including those SSTs discussed in our paper, are summarized in previous Waste Management presentations by Dodd [3-5]. After the wastes have been retrieved, the tanks will be filled with sand or other solid material to prevent collapse and covered to minimize human contact and infiltration of water [2]. The retrieved wastes will be processed into vitrified (glass) high-level and vitrified low-activity waste forms. In addition to these retrieved wastes, small amounts of residual waste (i.e., waste remaining after final retrieval operations) will remain in the storage tanks. Recovering all of the waste is not possible using available retrieval technologies. Most of the residual waste is expected to be on the bottom of each tank in a layer no more than an inch thick. Obtaining samples of this residual waste is difficult, because the selection of suitable sampling techniques is constrained by safety concerns related to their potential for damaging or piercing the tank bottom.

The residual wastes remaining in the tanks represent a potential future risk to groundwater quality if infiltrating water leaches contaminants from the residual wastes and transports them through the vadose zone to the groundwater. Estimating the future leaching of contaminants, such as Tc-99, U-238, I-129, and Cr, from these residual wastes requires detailed knowledge of the solids present in the waste, their major and trace element compositions, and their dissolution properties in the tank environment. Given the complexity of waste streams and tank-to-tank transfers from Hanford Site operations, contaminant source-term release models cannot be developed assuming analogies to the limited information available from Hanford tank simulant studies or previous analyses of sludge and supernatant samples taken prior to final retrieval from Hanford tanks. Therefore, characterization of actual residual waste is needed to develop the models that simulate contaminant release mechanisms from residual waste solids reacting with water infiltrating the tanks.

Several studies have been completed where wastes from various Hanford underground storage tanks were characterized by X-ray diffraction (XRD), scanning electron microscopy/energy dispersive X-ray spectroscopy (SEM/EDS), and/or transmission electron microscopy (TEM). These studies were based on wastes sampled prior to final sludge retrieval operations. Rapko and Lumetta [6] summarize results obtained through 1999 for the major solid phases identified in Hanford tank sludges, and Deutsch et al. [7] updated their tabulation to include more recently published data.

As part of its Residual Tank Waste Contaminant Release Project funded by CH2M HILL Hanford Group, Inc., the Pacific Northwest National Laboratory (PNNL) developed source-term models that describe the release of contaminants when infiltrating water or cement pore fluids contact residual waste solids. To date, PNNL has studied residual wastes from SSTs 241-C-103 (C-103) [8], 241-C-106 (C-106) [9,10], 241-C-202 (C-202) [11], 241-C-203 (C-203) [11], and 241-S-112 (S-112) [12]. As part of this same project, samples of tank waste taken prior to final retrieval from SSTs 241-BX-101 (BX-101) [13], 241-C-203 (C-203) [14-16], and 241-C-204 (C-204) [14-16], and DST 241-AY-102 (AY-102) [13] have also been tested and characterized.

PNNL is using a multi-tiered approach to study tank residual wastes. Tier 1 laboratory tests include determination of the inventory of contaminants and bulk constituents of the residual waste and quantification of the concentrations of leachable contaminants and other waste components. Leach tests

were conducted to evaluate contaminant leachability from the waste by infiltrating water or simulated cement pore waters. The leach tests were completed with deionized, $Ca(OH)_2$-saturated, and $CaCO_3$-saturated waters. The latter two solutions were used to mimic the pore fluid compositions associated with the initial and final status of a tank chemical system in which the void space above the residual waste is filled with a cementitious grout, a possible tank fill material. Based on the results of the Tier 1 tests, Tier 2 testing includes additional analyses that are completed to augment the initial characterization results and elucidate the controlling mechanism(s) for the release of contaminants. PNNL's approach is summarized in the companion Waste Management 2009 paper by Cantrell et al. [17]. Complete details and results of PNNL's Tier 1 and 2 studies of the residual wastes from these five SSTs are described in depth elsewhere [7-14,18,19]. All of the technical reports generated from this PNNL project are available online to the public in pdf format at http://www.pnl.gov/main/publications/.

The following paper focuses on the characterization of the compositions of the bulk residual waste solids and identification of the individual solid phases that are present in these wastes. The methods used for these analyses are briefly identified, and an overview of the results from testing and characterization of residual waste samples from SSTs C-103, C-106, C-202, C-203, and S-112 is presented. This paper also updates the earlier summary by Krupka et al. [20].

## SOLID-PHASE CHARACTERIZATION METHODS

### Tier 1 Characterization

A primary product of the tank waste testing is the measurement of the total contaminant concentrations in each residual waste sample. The elemental and contaminant concentrations of the wastes are measured directly on the solids and through the complete dissolution of the bulk residual waste solids using fusion-dissolution procedures and acid digestions. These methods are described in detail in Deutsch et al. [11]. The elemental and contaminant compositions of the bulk residual waste solids are then determined from the dissolved metal and contaminant concentrations and the total alpha and beta activities measured for these solutions using a combination of methods, including inductively coupled plasma-mass spectrometry (ICP-MS), inductively coupled plasma-optical emission spectroscopy (ICP-OES), and several radiochemical analytical techniques. Because the two solid digestion methods require the addition of acids to fully solubilize the waste solids, they are not appropriate techniques for determining the anion concentrations of the bulk residual waste. Anion concentrations of the bulk residual waste solids were estimated separately by adding results from sequential deionized water extracts of the bulk residual wastes [12]. The anion concentrations in these extracts are measured using ion chromatography (IC). This approach may underestimate the total quantities of anions in the sample, particularly for anions that can form insoluble precipitates.

### Tier 2 Characterization

Tier 2 characterization analyses typically consist of XRD and SEM/EDS analyses to identify individual phases that make up the residual wastes and any discrete phases that may contain contaminants. In some cases, additional studies are done based upon the specific characteristics of particular residual waste samples determined in Tier 1 analyses. Tier 2 activities have included solubility tests, selective extractions, and application of synchrotron-based X-ray techniques and Mössbauer spectroscopy.

Standard powder (bulk) XRD techniques are used to identify the crystalline phases present in the unleached (i.e., as-received) residual waste samples and leached solids remaining after the various residual waste leaching and selective extraction tests (see companion paper by Cantrell et al. [17]). The sample handling methodology, XRD instrumentation, and procedures used for data reduction and examination are described elsewhere [8]. Of particular note is the use of disposable XRD specimen

holders designed at PNNL specifically for the safe handling of powders containing highly radioactive or hazardous dispersible materials [21]. X-ray diffraction cannot be used to characterize amorphous or poorly crystalline phases, and is not sensitive to trace concentrations of a particular crystalline solid. As a general rule, a crystalline phase must be present at greater than ~5 to 10 wt% of the total sample mass to be readily detected by XRD.

Scanning electron microscopy in combination with EDS and element mapping techniques are used to characterize the phase associations, morphologies, particle sizes, surface textures, and compositions of solid particles in the unleached and leached residual waste samples. Scanning electron microscopy is an electron beam imaging technique used to obtain high-resolution photomicrographs at the submillimeter to submicrometer size scale to characterize the morphologies (e.g., size and shape) of individual solid particles and particle aggregates and any surface coatings or interstitial matrix material that may be associated with these solids. Energy dispersive X-ray spectroscopy, which is auxiliary detector instrumentation on an SEM and some transmission electron microscopes (TEMs), is used for qualitative determination of the elemental composition of selected locations of particles under examination with the SEM. The SEM/EDS instrumentation and operating conditions used for the studies of residual waste are described elsewhere [8]. To help identify particles that contain elements with large atomic numbers, such as Tc or U, the SEM is operated in the backscattered electron (BSE) emission mode. The intensity of features in the BSE photomicrograph is a function of the element's atomic number – the larger the atomic number, the brighter the signal. For each sample, one or more photomicrographs are first recorded at low magnification for a representative area of the mount to provide a general perspective of the sizes, types, and distributions of particles that make up each sample. Additional SEM micrographs are then recorded of particles at greater magnifications to provide a more detailed representation of the particles' characteristics, and selected points on these particles are then analyzed by EDS.

We have also demonstrated the feasibility of using synchrotron-based X-ray analysis methods and Mössbauer spectroscopy for Tier 2 characterization of tank residual solids [7]. The synchrotron-based X-ray analyses were completed on beamline ID-20 (PNC-CAT) at the Advanced Photon Source (Argonne National Laboratory, Argonne, Illinois), and included X-ray absorption spectroscopy (XAS), such as X-ray absorption near edge structure (XANES) and extended X-ray absorption fine structure (EXAFS) spectroscopy; micro X-ray fluorescence (μSXRF); and micro X-ray diffraction (μXRD). The XANES and EXAFS analyses are used to provide information about the oxidation state and chemical bonds for certain elements in solid and solution samples. Micro X-ray fluorescence is used for mapping the distribution of element concentrations in samples at the micrometer to submicrometer scale, and is particularly sensitive for elements with large atomic numbers, such as U and Tc. Micro X-ray diffraction is used to identify crystalline solid phases at the micrometer to submicrometer scale. Mössbauer spectroscopy has been used to identify the composition and abundance of Fe-containing phases in tank residual waste. These techniques have received limited use in our testing protocol because of difficult scheduling requirements and other priorities for project resources. Moreover, because residual waste samples are highly radioactive dispersible powders, specialized containment protocols must be followed when handling and preparing the samples. Additionally, specialized sample mounts that control dispersibility are typically required in order analyze residual waste samples at offsite locations.

Other analytical techniques have been considered as part of the Tier 2 testing, but have not been used to date because of project information priorities, resource issues, and sample handling and preparation requirements. These techniques include TEM, electron microprobe (EMP) analysis, and X-ray photoelectron spectroscopy (XPS).

## RESULTS AND DISCUSSION

The following discussion focuses on general findings pertaining to the solid-phase characteristics of residual waste from the SSTs C-103, C-106, C-202, C-203, and S-112. A detailed description of the testing methods and characterization results are provided in technical reports and journal publications cited previously. Deutsch et al. [19] provide a compendium of the results from our studies of C-103, C-106, C-202, and C-203 residual wastes. Analyses of residual waste from S-112 are described in Cantrell et al. [12].

The results indicate that the compositions and contaminant concentrations of the bulk residual wastes and solid phases vary between the different SSTs. These differences undoubtedly result from the various waste types stored and transferred into and out of each tank and the different sluicing and retrieval operations used for waste retrieval. The potential for such differences is readily apparent simply from a visual inspection of the samples used for testing and analysis (Fig. 1). For comparison purposes, Table I lists the concentrations of elements and contaminants typically present at detectable levels in bulk residual waste from C-103, C-106, C-202, and C-203, and S-112 as determined from acid digestion. The concentrations of most elements, including the main waste constituents such as Al, Fe, and Na, differ appreciably between these five residual wastes (Table I). The concentrations of Ca and Mn in the residual waste from C-106 are also significantly greater than those for the other four residual wastes. Based on the XRD and SEM/EDS analyses for the C-106 solids, the higher Ca and Mn concentrations are likely due to the oxalic acid dissolution treatment used for C-106 waste retrieval [3]. Residual wastes from C-106, C-202, and C-203 were also analyzed by the fusion-dissolution method described previously. The reader is referred to Deutsch et al. [10,11] for a comparison of the compositions determined by fusion-dissolution versus acid digestion for the bulk residual waste from these three SSTs.

Studies of tank waste from C-203 taken before and after final retrieval [11,14] indicate that the composition of the final residual waste can also differ significantly from that of waste taken prior to retrieval. Comparison of the bulk compositions of C-203 pre-retrieval waste and post-retrieval residual wastes shows that the concentrations of Cr (17,900 µg/g dry wt.), Fe (52,000 µg/g dry wt.), and Na (160,000 µg/g dry wt.) in the pre-retrieval waste are significantly greater than those in the final residual


Fig. 1. Photographs of the as-received samples of C-103 (subsample 19849), C-203 (subsample 19961), and S-112 (subsample 20407) residual wastes [8,11,12].

Table I. Average Elemental and Contaminant Compositions of the Bulk Residual Waste from C-103, C-106, C-202, and C-203, and S-112 as Determined by Acid Digestion [8,10-12].

| Analyte | C-103 | C-106 | C-202 | C-203 | S-112 |
|---|---|---|---|---|---|
| | (µg/g dry wt.) | | | | |
| Al | 136,000 | 81,700 | 13,600 | <710 | 291,000 [a] |
| Ba | 181 | 914 | 208 | <142 | 12.6 |
| Ca | 616 | 46,500 | 14,500 | 3,140 | 56.9 |
| Cr | 193 | (727) [b] | 13,200 | 5,910 | 1,730 |
| Fe | 12,000 | 36,700 | 122,000 | 16,300 | 2,280 |
| K | BDL [c] | 8,530 | <15,800 | <355,000 | 68.9 |
| Mg | (42) | 3,160 | 2,560 | (729) | 4.82 |
| Mn | 470 | 108,000 | 25,700 | 956 | 14.4 |
| Na | 7,840 | 46,700 | 58,800 | 95,800 | 49,100 |
| Ni | 420 | 5,370 | 9,070 | 510 | 9.01 |
| Pb | 892 | 4,810 | 7,980 | 5,630 | 7.11 |
| Si | 9,070 | (4,900) | 25,000 | 3,490 | 1,220 |
| Sr | 90.7 | (493) | 1,510 | 409 | 4.02 |
| U-238 | 3,730 | 310 | 207,000 | 505,000 | 23.8 |
| Pu-239 | 8.02 | 27.7 | 435 | 18.2 | NA |
| Np-237 | 1.30 | 9.04 | 2.16 | (0.0519) | NA |
| Am-241 | 0.053 | 2.05 | 0.449 | 0.0140 | NA |
| Tc-99 | 0.231 | 1.14 | 0.149 | (0.0947) | 0.474 |
| I-129 | ($1.11 \times 10^{-5}$) | NA | NA | NA | NA |

[a] The Al concentration listed above for S-112 is that reported by analyses completed by Hanford's 222-S Laboratory. It was assumed that the 222-S Laboratory result for Al is correct, because it is consistent with the XRD results which indicates the solid is essentially all gibbsite [$Al(OH)_3$]. The average Al concentration determined by Cantrell et al. [12] was 77,200 µg/g dry wt. and was much lower than expected. The reason for this discrepancy is being evaluated.

[b] Values in parentheses were less than the estimated quantification limit (EQL).

[c] BDL = Below detection limit.

[d] NA = Not analyzed .

waste (see composition of C-203 residual waste in Table I). On the other hand, retrieval operations resulted in an increase in the concentration of U-238 per unit mass of bulk waste from 195,000 µg/g dry wt. in the pre-retrieval waste to 505,000 µg/g dry wt. in the final residual waste. Testing of the pre-retrieval C-203 waste showed that the majority of U is in the form of čejkaite [$Na_4(UO_2)(CO_3)_3$] and a minor fraction in the form of clarkeite [$Na(UO_2)O(OH)(H_2O)_{0-1}$] or $Na_2U_2O_7 \cdot xH_2O$ [14]. It is assumed that the retrieval process, which utilized water to enhance sludge removal [4], may have preferentially removed the relatively soluble čejkaite and therefore caused the enrichment of the more recalcitrant clarkeite or $Na_2U_2O_7 \cdot xH_2O$, thus increasing the U concentration per unit mass of the final residual waste.

The studies show the residual waste samples to be complex in terms of the types of solid phases present in the bulk solid and the various morphologies, textures, and crystallinities exhibited by the individual solid phases. For example, Fig. 2 shows a series of SEM micrographs of solids present in unleached C-103

residual waste. These micrographs clearly show the complexity of the morphologies and textures exhibited by some of the residual waste samples studied to date. Table II shows the extensive assemblage of different solid phases identified by XRD and SEM/EDS in samples of unleached and leached C-103 residual waste. Particles present in unleached and leached samples are typically very small in size (from several tens of micrometers to submicrometer), and appear to be amorphous, coated with other phases, and/or aggregated as a complex assemblage of submicrometer-size particles. Depending on the specific SST, numerous crystalline solids {such as gibbsite [$Al(OH)_3$]; böhmite [AlO(OH)]; cancrinite [$Na_6CaAl_6Si_6(CO_3)O_{24}\cdot 2H_2O$]; dawsonite [$NaAlCO_3(OH)_2$]; Fe oxides such as hematite ($\alpha$-$Fe_2O_3$), goethite [$\alpha$-FeO(OH)], and maghemite ($\gamma$-$Fe_2O_3$); rhodochrosite ($MnCO_3$); lindbergite ($MnC_2O_4\cdot 2H_2O$); whewellite ($CaC_2O_4\cdot H_2O$); and nitratine ($NaNO_3$)} have been identified by XRD in residual wastes from one or more of the five SSTs studied to date. In addition to the crystalline phases listed above, numerous other solid phases were identified by SEM/EDS (for example, see Table II), which have compositions that do not correspond to any of the crystalline phases. Such phases are likely present in too low of concentrations or are amorphous and therefore cannot be detected by XRD analysis of the bulk residual

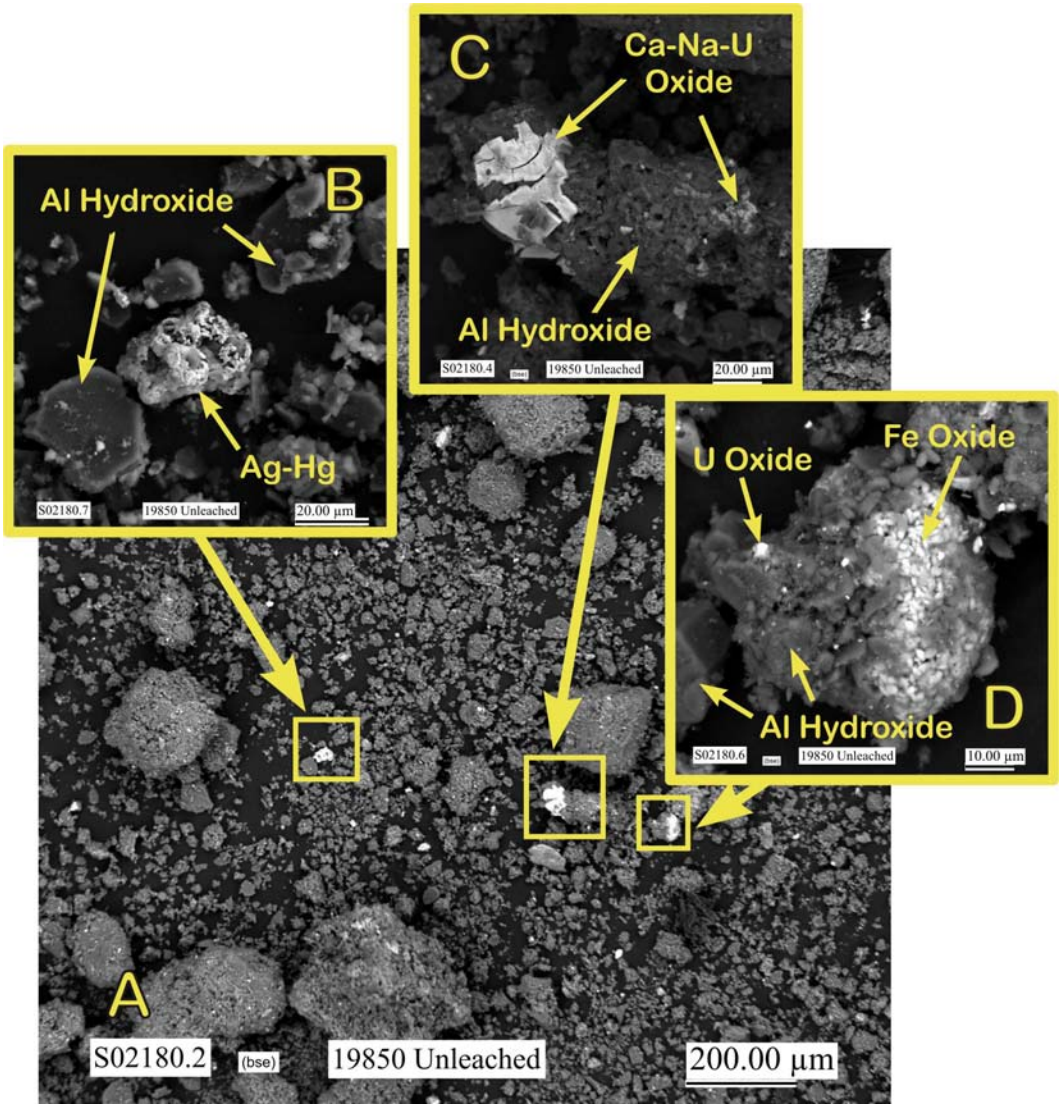

Fig. 2. Low (A) and high (B, C, and D) magnification SEM micrographs collected using backscattered electron (BSE) emission of typical solids present in unleached C-103 residual waste (subsample 19850) [8].

Table II. Summary of Phases Indicated by SEM/EDS and XRD Results for Unleached and Leached Samples of C-103 Residual Waste [8]. [Because H is not detectable by EDS and C was used for coating the SEM mounts, all of the phases listed below as being identified by SEM/EDS may also contain H and/or C.]

| Compositions of Phases Identified by SEM/EDS | Phases Identified by XRD that Correspond to Those Detected by SEM/EDS | Information Regarding Occurrence Based on SEM/EDS Analyses |
|---|---|---|
| Al – O | gibbsite | Most dominant phase in all unleached and leached samples; possibly two Al-OH phases based on EDS |
| Fe – O | hematite | Second most common phase; present in all unleached and leached samples; two Fe oxyhydroxides phases may be present based on morphology; Cr, Ni, Pb, and Mn are always associated with these phases |
| Ag ± Hg – O | | Present in all unleached and leached samples; two Ag phases may present - Ag oxide (with no detectable Hg) and Ag-Hg oxide |
| U – O | | Most common U-containing particle; typically present as micrometer- or submicrometer-sized particles |
| Na – Ca – Al – Si – O | cancrinite – identified by XRD only in the $Ca(OH)_2$-leached subsample 19845 | Morphology similar to "balls of twine," which is similar to the crystal habit identified by others as the mineral cancrinite |
| Ca – P – O | | Present in the unleached, deionized water-leached, $CaCO_3$-leached, and possibly the $Ca(OH)_2$-leached samples |
| Na – Ca – U – O | | Rare; identified in unleached residual waste samples |
| Si – Al – Mg – Na – Fe – O | | Rare |
| Na – S – O | | Rare; identified in deionized water-leached samples |
| Zr – O | | Rare; identified in unleached and $CaCO_3$-leached samples |
| Th – O | | Rare; identified in $CaCO_3$-leached samples |
| Fe – Pb - O | | Identified in deionized water-leached samples |
| Ca – O | | Phase identified in 1-month single-contact $Ca(OH)_2$-leached samples; common phase; has well-formed crystal faces; EDS composition agrees with that of $CaCO_3$ |
| Ca – Al – Si – O | | Phase identified in 1-month single-contact $Ca(OH)_2$-leached samples; common phase; has platy crystal habit; platy crystals often form clusters; angles on corners of platelets appear |

| | | |
|---|---|---|
| | | to be ~120° |
| Ca – Al – O | katoite (or hydrogrosslarite) $Ca_3Al_2(OH)_{12}$ | Phase identified in 1-month single-contact $Ca(OH)_2$-leached samples; appears to be spherical intergrowth of interlocking cubic crystals |
| | $Ca_4Al_2O_6CO_3 \cdot 11H_2O$ | Phase identified in 1-month single-contact $Ca(OH)_2$-leached samples |
| | rabejacite $Ca(UO_2)_4(SO_4)_2(OH)_6 \cdot 6H_2O$ | Phase identified in 1-month single-contact $Ca(OH)_2$-leached samples |

waste. Although crystalline phases were identified in residual waste from C-103, C-106, and S-112, no crystalline phases were detected by XRD in the bulk residual waste samples from C-202 and C-203. This suggests that 90% or more of the C-202 and C-203 residual wastes are made up of amorphous or poorly crystalline solid phases.

At least two oxalate compounds, lindbergite and whewellite, were identified in the C-106 residual waste. Because these two oxalates were not identified in the other residual waste samples, they likely resulted from the use of the oxalic acid dissolution and modified sluicing method for C-106 waste retrieval. The presence of oxalate solid(s) is consistent with the laboratory studies of C-106 pre-retrieval waste by Bechtold et al. [22]. They identified hematite, gibbsite, böhmite, possibly "Mn(II) oxalate" ($MnC_2O_4 \cdot 2H_2O$), and traces of Nd-rich and Pb-rich particulates in residue from C-106 pre-retrieval waste reacted with 1 M oxalic acid. These compounds match up with phases identified in the PNNL studies of C-106 residual waste. However, several compounds (e.g., dawsonite, rhodochrosite, whewellite, one or two Ag-Hg phases, and several phases containing Si) observed in our studies do not correspond to any phases identified by Bechtold et al. [22]. Some of these phases that may be amorphous and/or present at concentrations too low for detection in the samples studied by Bechtold et al. [22].

The primary contaminants of concern in the residual wastes are typically U-238, Cr, I-129, and Tc-99 because of their mobility in the environment and, for the radioactive elements, their long half-lives. Analyses of the bulk residual wastes (Table I) indicate that these contaminants are present at detectable concentrations in all or most the SST residual wastes. However, it was not always possible to identify some of these contaminants by EDS or XRD in samples of unleached or leached residual waste. This is likely due to the low concentrations (i.e., less than a few micrograms per gram of residual waste) of these contaminants, especially I-129 and Tc-99, in the residual wastes. Although XRD analyses have not identified any crystalline U-containing particles in the five residual wastes studied to date, the EDS studies did find U-containing particles in residual wastes from C-103, C-202, and C-203, but not C-106 or S-112. As a general rule, a crystalline phase must be present at greater than ~5 to 10 wt% of the total sample mass to be readily detected by XRD. As noted previously, C-202 and C-203 residual wastes were unusual in that they contained mostly X-ray amorphous (non-crystalline) solids. Of the residual wastes studied to date, the bulk samples of C-103, C-202, and C-203 residual wastes also contained the highest concentrations of U-238 (see Table I). The EDS analyses indicate the presence of U oxide/hydroxide and possibly Na-Ca-U oxide/hydroxide particles in C-103, and a U-Na-C-O-P phase in the C-202 and C-203 residual wastes. For comparison, the XRD and EDS studies reveal the presence of čejkaite [$Na_4(UO_2)(CO_3)_3$] and a Na-U oxide, possibly poorly crystalline $Na_2U_2O_7$ {or clarkeite $Na[(UO_2)O(OH)](H_2O)_{0-1}$}, in pre-retrieval waste from C-203 [14,15]. Essentially all Cr detected by EDS in samples we have studied to date is associated (i.e., coprecipitated) with Fe and Fe/Mn-oxide/hydroxide phases. Although I-129 and Tc-99 are present in the residual wastes, I-129 and until recently Tc-99 have not be detected in any particles analyzed by EDS. Given the low solubility of AgI compounds, Hg-Ag particles identified in C-103 and C-106 residual wastes are possible hosts for sequestration of I-129. Some of the selective extraction results suggested that Tc-99 is likely associated with the Fe-oxide/hydroxide phases [10]. Until recently, we had not detected Tc-containing phases by XRD or EDS in any SST pre-retrieval tank waste or post-retrieval residual waste samples. In the study by Cantrell et al. [8], we identified Tc by EDS in three Fe oxide/hydroxide particles in samples of unleached, deionized water-leached, and $CaCO_3$-leached C-103 residual waste. The Tc concentrations in these particles ranged from ~0.6 to ~1.0 wt%. We believe this to be the first direct evidence of Tc in solid phases in actual samples of pre-retrieval or residual wastes from Hanford SSTs. Although others [23,24] have proposed that Al oxide/hydroxide phases are possible candidates as hosts for coprecipitation of Tc-99 in tank wastes, we have never detected Tc-99 in any of the hundreds of Al oxide/hydroxide particles examined by EDS.

The studies also demonstrate that contact of residual wastes with $Ca(OH)_2$- and $CaCO_3$-saturated solutions, which were used as surrogates for the compositions of pore-fluid leachants derived from young and aged cements, respectively, may alter the compositions of solid phases present in the contacted wastes. X-ray diffraction and SEM/EDS analyses of $Ca(OH)_2$- and $CaCO_3$-leached samples show the presence of Ca-containing particles, such as calcite ($CaCO_3$), which were not observed in the unleached and water-leached samples of these residual wastes [8,9,11]. For C-103 residual wastes [8], additional Ca-containing phases, such as phases Ca-O (probably calcite), Ca-Al-Si-O, katoite, Ca-Al-O-$CO_3$ hydrate, and rabejacite (all listed near the bottom of Table II), were identified by SEM/EDS or XRD in the $Ca(OH)_2$- and $CaCO_3$-leached samples and not the unleached and water-leached samples.

Fig. 3 shows a ternary plot for the concentrations [at.%] of U, Na, and Ca normalized to a total of 100% for all U-Na-C-O-P particles analyzed by EDS in aliquots of unleached, water-leached, $Ca(OH)_2$-leached, and $CaCO_3$-leached C-203 residual waste (subsample 19961) [11]. Ternary (or triangle) plots are commonly used to illustrate differences in chemical compositions of complex systems. A ternary plot graphically depicts relative percentages (or ratios) of three variables (e.g., U, Na, and Ca) as positions in an equilateral triangle. The proportions of the three variables sum to a constant value such as 1.0 or 100%. Each side of the triangle represents the proportions from 0 to 100% of two of the three variables.

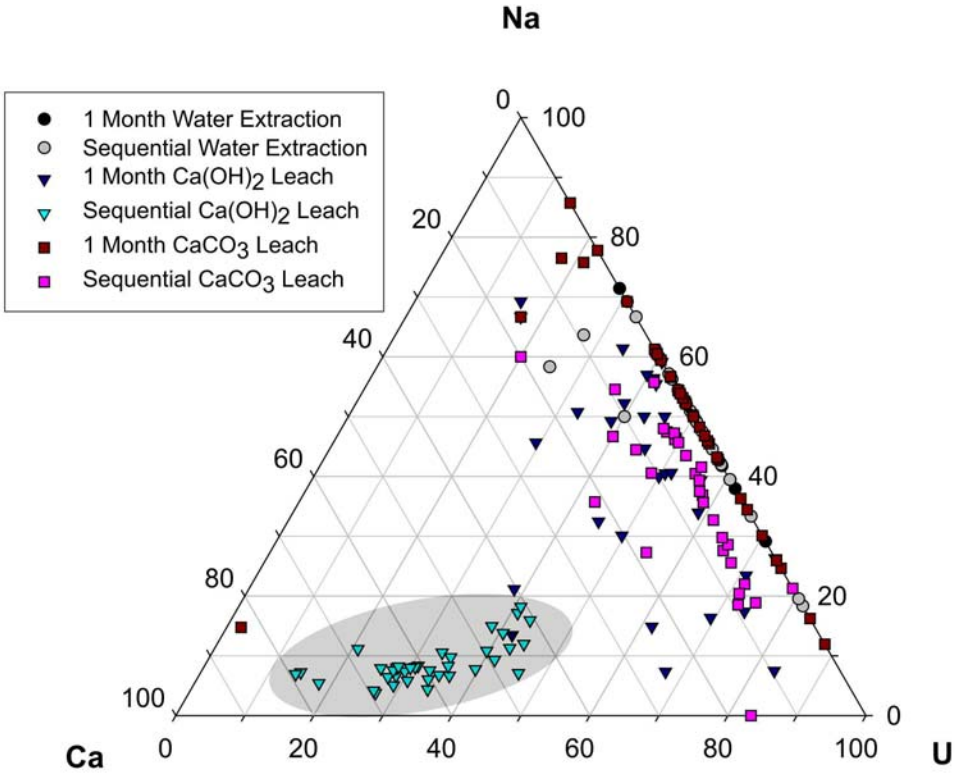


Fig. 3. Ternary plot of the EDS-determined Na-U-Ca concentrations (at.%) normalized to 100% for U-Na-C-O-P particle aggregates present in unleached, water-leached, $Ca(OH)_2$-leached, and $CaCO_3$-leached samples of C-203 residual waste (subsample 19961) [11].

A sample containing only two of the three variables will plot along one of the three sides of the triangle. As the proportion of the third variable increases in a sample, the point representing that sample moves from the side of the triangle to the opposite point of the triangle. The EDS results in Fig. 3 indicate that the U-Na-C-O-P particle aggregates from the 1-month single-contact and sequential $Ca(OH)_2$-leached and sequential $CaCO_3$-leached samples (dark blue triangles, light blue triangles, and light red squares in Fig. 3, respectively) contain significantly more Ca and less Na. This is especially apparent for analyses of particles from the sequential $Ca(OH)_2$-leached samples (gray shaded area in Fig. 3). This increase in Ca concentrations relative to Na is consistent with the results for $Ca(OH)_2$- and $CaCO_3$-leached samples of C-203 residual sludge. Unfortunately, the mechanism responsible for this shift in particle compositions has not been determined.

Of particular interest is the presence of Fe oxides/hydroxides that exist in these residual wastes as discrete particles, particles intergrown within a matrix of other phases, and surface coatings on other particles or particle aggregates. Iron oxides/hydroxides have been identified by XRD and SEM/EDS in residual wastes from all five SSTs. These Fe oxides/hydroxides typically contain trace concentrations of other transition metals, such Cr, Mn, Ni, and/or Pb. Coprecipitation of Mn with the Fe oxides/hydroxides is especially evident for the residual waste from C-106 which contained high Mn concentrations (see Table I) [9,10]. SEM/EDS examination revealed the presence of Fe oxide/hydroxide coatings on particles in many of the residual wastes (Fig. 4). If any contaminant-containing solids are coated by or incorporated into the Fe oxides/hydroxides or reaction products precipitated from contact with cement pore fluids, they would be isolated to various degrees from fluids that enter the SSTs and react with the remaining residual wastes. The dissolution of contaminant-containing particles coated by Fe oxides/hydroxides (or any other phases such as calcite) would be delayed until these coatings had dissolved sufficiently to expose the underlying matrix to infiltrating pore fluids.

Synchrotron-based analyses have also been completed for a limited number of tank waste samples, including C-106 residual waste and C-203 pre-retrieval tank waste [7]. Synchrotron-based analyses allow solid-phase identification on a much smaller (micrometer) scale, while also providing the capability to characterize the oxidation states and compositions of the solid phases. Samples of water-leached C-203 pre-retrieval waste were studied by synchrotron-based μXRD to help identify U-containing phases that could not be positively identified by bulk XRD. Diffraction patterns were collected by μXRD on ~5 μm diameter areas of U-rich regions in the waste sample, which were first located by μSXRF analyses. The μXRD results were consistent with the presence of clarkeite and/or $Na_2U_2O_7$, as well as with goethite and maghemite which had not been identified previously by bulk XRD [7]. The μSXRF, XANES, and EXAFS analyses of C-106 residual waste indicated that Ag, Cr, Fe, Mn, and U were present in the waste solids primarily in the 0 (metallic), +3, +3, +2, and +6 oxidation states, respectively [7]. These analyses also showed that a small fraction of U was present as U(IV), and the results for Mn were also consistent with the possible presence of a Mn(III) phase.

## CONCLUSIONS

Studies of residual wastes completed to date show significant variability in the compositions of these wastes and the chemistries, morphologies, and crystallinities of the individual phases present in the wastes. Therefore, contaminant source-term release models for tank residual wastes cannot be developed assuming analogies to the limited information available from Hanford tank simulant studies or previous analyses of sludge and supernatant samples taken prior to final retrieval from Hanford tanks. Characterization of actual residual waste is needed to develop the models that simulate contaminant release mechanisms from residual waste solids reacting with water infiltrating the tanks in the future. Because these wastes are highly radioactive and chemically complex assemblages of solids that contain contaminants as discrete phases and/or sequestered within other phases, their detailed characterization presents an extraordinary challenge.

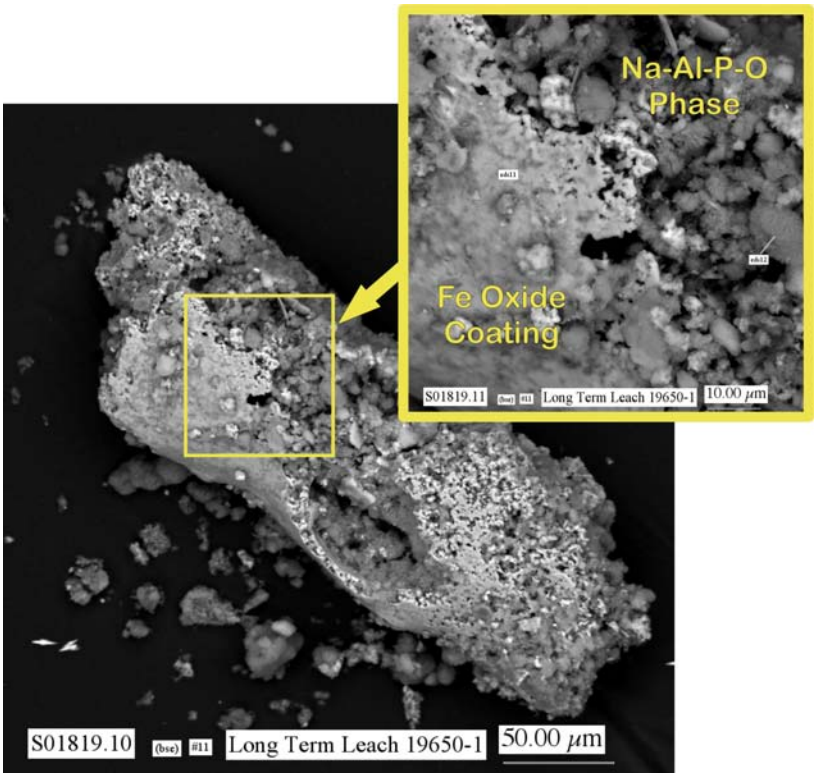


Fig. 4. Backscatter SEM Micrographs of Fe oxide/hydroxide coating on particle aggregate present in water-leached, pre-retrieval tank waste from SST C-204 (subsample 19650) [14,15].

Certain key cross-cutting geochemical processes and solid phase characteristics important to contaminant waste release are becoming evident, now that residual wastes have been studied from several SSTs. For example, the characterization results suggest that Fe oxide/hydroxide phases, which are often present as coatings or intergrown within an aggregate of other phases in residual waste, likely play an important role relative to the long term stability of residual waste and release of certain contaminants, such as Cr and possibly Tc. Understanding the chemistry and dissolution rates of the coprecipitated forms of Fe oxides/hydroxides would provide a mechanistic approach to estimating release rates for Cr and Tc.

Certain aspects of our approaches to solid-phase characterization have turned out to be valuable with respect to improving the interpretation and integration of the solid-phase characterization results. These approaches, such as doing SEM/EDS analyses in BSE emission mode, completing XRD-SEM/EDS studies in an iterative fashion, and using EDS elemental mapping techniques, are discussed in Krupka et al. [20].

As residual tank wastes from more SSTs are characterized in terms of composition and contaminant release, it is anticipated that common characteristics with respect to the type of waste stored in the tank will become evident. This may allow the grouping of tanks into general categories with certain common chemical features and contaminant release characteristics – an important goal because complete characterization of residual wastes from all 149 SSTs is not practical. Moreover, the resulting mechanistic source-term models will be more scientifically defensible and less conservative, which may reduce the costs of tank-farm closure.

**ACKNOWLEDGMENTS**

The authors acknowledge M. Connelly and F. M. Mann at CH2M HILL Hanford Group, Inc. (Richland, WA) for providing project funding and technical guidance. The quality of the manuscript was greatly improved from review comments received from H. Babad (private consultant, Richland, Washington) and C. F. Brown (PNNL). We also want to express our appreciation to PNNL management who provided funding to support our presentations and attendance at the Waste Management 2009 conference. Pacific Northwest National Laboratory is operated for the DOE by Battelle Memorial Institute under Contract DE-AC05-76RL01830. Synchrotron-based analyses were completed at the PNC CAT project at the Advanced Photon Source; the PNC CAT project is supported by funding from the U.S. Department of Energy Basic Energy Sciences, the University of Washington, Simon Fraser University, and the Natural Sciences and Engineering Research Council (NSERC) of Canada. Use of the Advanced Photon Source is supported by the U. S. Department of Energy, Office of Science, Office of Basic Energy Sciences, under Contract DE-AC02-06CH11357.

**REFERENCES**

[1] M. N. JARAYSI, J. G. KRISTOFZSKI, M. P. CONNELLY *et al.*, "Initial Single-Shell Tank System Performance Assessment for the Hanford Site," *Proceedings of the 33th International Waste Management Conference (WM'07), February 25 - March 1, 2007, Tucson, Arizona*, Paper 7359, Tucson, Arizona: WM Symposia, Inc. (2007).

[2] DOE/ORP, (U.S. Department of Energy, Office of River Protection), *Initial Single-Shell Tank Performance Assessment for the Hanford Site,* DOE/ORP-2005-01, U.S. Department of Energy, Office of River Protection, Richland, Washington (2006).

[3] R. A. DODD, and J. W. CAMMANN, "Progress in Retrieval and Closure of First High-Level Waste Tank at Hanford: Single Shell Tank C-106," *Proceedings of the 31th International Waste Management Conference (WM'05), February 27 - March 3, 2005, Tucson, Arizona*, Session 20, Paper 6, Tucson, Arizona: WM Symposia, Inc. (2005).

[4] R. A. DODD, "Tank Waste Retrieval Lessons Learned at the Hanford Site," *Proceedings of the 32th International Waste Management Conference (WM'06), February 26 - March 2, 2006, Tucson, Arizona*, Session 73, Paper 7, Tucson, Arizona: WM Symposia, Inc. (2006).

[5] R. A. DODD, *Tank Waste Retrieval Lessons Learned at the Hanford Site,* CH2M-36346-FP, CH2M Hill Hanford Group, Inc., Richland, Washington (2008).

[6] B. M. RAPKO, and G. J. LUMETTA, *Status Report on Phase Identification in Hanford Tank Sludges,* PNNL-13394, Pacific Northwest National Laboratory, Richland, Washington (2000).

[7] W. J. DEUTSCH, K. M. KRUPKA, K. J. CANTRELL *et al.*, *Advances in Geochemical Testing of Key Contaminants in Residual Hanford Tank Waste,* PNNL-15372, Pacific Northwest National Laboratory, Richland, Washington (2005).

[8] K. J. CANTRELL, K. M. KRUPKA, W. J. DEUTSCH *et al.*, *Hanford Tank 241-C-103 Residual Waste Contaminant Release Models and Supporting Data,* PNNL-16738, Pacific Northwest National Laboratory, Richland, Washington (2008).

[9] W. J. DEUTSCH, K. M. KRUPKA, M. J. LINDBERG *et al.*, *Hanford Tank 241-C-106: Impact of Cement Reactions on Release of Contaminants from Residual Waste,* PNNL-15544, Pacific Northwest National Laboratory, Richland, Washington (2006).

[10] W. J. DEUTSCH, K. M. KRUPKA, M. J. LINDBERG *et al.*, *Hanford Tank 241-C-106: Residual Waste Contaminant Release Model and Supporting Data,* PNNL-15187, Rev. 1, Pacific Northwest National Laboratory, Richland, Washington (2007).

[11] W. J. DEUTSCH, K. M. KRUPKA, M. J. LINDBERG *et al.*, *Hanford Tanks 241-C-202 and 241-C-203 Residual Waste Contaminant Release Models and Supporting Data,* PNNL-16229, Pacific Northwest National Laboratory, Richland, Washington (2007).

[12] K. J. CANTRELL, K. M. KRUPKA, K. N. GEISZLER *et al.*, *Hanford Tank 241-S-112 Residual Waste Composition and Leach Test Data,* PNNL-15793, Pacific Northwest National Laboratory, Richland, Washington (2008).

[13] K. M. KRUPKA, W. J. DEUTSCH, M. J. LINDBERG *et al.*, *Hanford Tanks 241-AY-102 and 241-BX-101: Sludge Composition and Contaminant Release Data,* PNNL-14614, Pacific Northwest National Laboratory, Richland, Washington (2004).

[14] W. J. DEUTSCH, K. M. KRUPKA, M. J. LINDBERG *et al.*, *Hanford Tanks 241-C-203 and 241-C-204: Residual Waste Contaminant Release Model and Supporting Data,* PNNL-14903, Pacific Northwest National Laboratory, Richland, Washington (2004).

[15] K. M. KRUPKA, H. T. SCHAEF, B. W. AREY *et al.*, "Residual Waste from Hanford Tanks 241-C-203 and 241-C-204. 1. Solids Characterization," *Environmental Science and Technology,* vol. 40, no. 12, pp. 3749-3754 (2006).

[16] K. J. CANTRELL, K. M. KRUPKA, W. J. DEUTSCH *et al.*, "Residual Waste from Hanford Tanks 241-C-203 and 241-C-204. 2. Contaminant Release Model," *Environmental Science and Technology,* vol. 40, no. 12, pp. 3755-3761 (2006).

[17] K. J. CANTRELL, K. M. KRUPKA, W. J. DEUTSCH *et al.*, "Contaminant Release from Residual Waste in Hanford Single Shell Tanks at the Hanford Site, Washington, USA," *Proceedings of the 35th International Waste Management Conference (WM'09), March 1- 5, 2009, Phoenix, Arizona*, Paper 9276, Tucson, Arizona: WM Symposia, Inc. (2009).

[18] M. J. LINDBERG, and W. J. DEUTSCH, *Tank 241-AY-102 Data Report,* PNNL-14344, Pacific Northwest National Laboratory, Richland, Washington (2003).

[19] W. J. DEUTSCH, K. J. CANTRELL, and K. M. KRUPKA, *Contaminant Release Data Package for Residual Waste in Single-Shell Hanford Tanks,* PNNL-16748, Pacific Northwest National Laboratory, Richland, Washington (2007).

[20] K. M. KRUPKA, W. J. DEUTSCH, H. T. SCHAEF *et al.*, "Characterization of Solids in Residual Wastes from Underground Storage Tanks at the Hanford Site, Washington, U.S.A.," *Scientific Basis for Nuclear Waste Management XXX*, Symposium Proceedings vol. 985, D. S. Dunn, C. Poinssot and B. Begg, eds., pp. 473-482, Warrendale, Pennsylvania: Materials Research Society (2007).

[21] D. M. STRACHAN, H. T. SCHAEF, M. J. SCHWEIGER *et al.*, "A Versatile and Inexpensive XRD Specimen Holder for Highly Radioactive or Hazardous Specimens," *Powder Diffraction,* vol. 18, no. 1, pp. 23-28 (2003).

[22] D. B. BECHTOLD, G. A. COOKE, D. L. HERTING *et al*., *Laboratory Testing of Oxalic Acid Dissolution of Tank 241-C-106 Sludge*, RPP-17158, Rev. 0, Fluor Hanford, Inc. Richland, Washington (2003).

[23] B. WAKOFF, and K. L. NAGY, "Perrhenate Uptake by Iron and Aluminum Oxyhydroxides: An Analogue for Pertechnetate Incorporation in Hanford Waste Tank Sludges," *Environmental Science and Technology,* vol. 38, no. 6, pp. 1765-1771 (2004).

[24] P. C. ZHANG, J. L. KRUMHANSL, and P. V. BRADY, "Boehmite Sorbs Perrhenate and Pertechnetate," *Radiochimica Acta,* vol. 88, no. 6, pp. 369-373 (2000).